



Risk and the Point of No Return for Climate Action

Matthias Aengenheyster¹, Qing Yi Feng², Frederik van der Ploeg³, and Henk A. Dijkstra²

¹Atmospheric, Oceanic and Planetary Physics, Department of Physics, Oxford University, Oxford, UK

²Institute for Marine and Atmospheric Research Utrecht, Department of Physics, Utrecht University, Utrecht, the Netherlands

³Centre for the Analysis of Resource Rich Economies, Department of Economics, Oxford University, Oxford, UK

Correspondence to: H.A. Dijkstra (H.A.Dijkstra@uu.nl)

Abstract. If the Paris targets are to be met, there may be very few years left for policy makers to start cutting emissions. Here, we ask by what year at the latest one has to take action to keep global warming below the 2 K target (relative to preindustrial levels) at the year 2100 with a 67% probability; we call this the Point of No Return (PNR). Using a novel, stochastic model of CO₂ concentration and global mean surface temperature derived from the CMIP5 ensemble simulations, we find that cumulative CO₂ emissions from 2015 onwards may not exceed 424 GtC and that the PNR is 2035 for the policy scenario where the share of renewable energy rises by 2% per year. Pushing this increase to 5% per year delays the PNR until 2045. For the 1.5 K target, the carbon budget is only 198 GtC and there is no time left before starting to increase the renewable share by 5% per year. If the risk tolerance is tightened to 5%, the PNR is brought forward to 2022 for the 2 K target and has been passed already for the 1.5 K target. Including substantial negative emissions towards the end of the century delays the PNR from 2035 to 2042 for the 2 K and to 2026 for the 1.5 K target, respectively. We thus show the impact on the PNR not only of the temperature target and the speed by which emissions are cut, but also of risk tolerance, climate uncertainties and the 10 potential for negative emissions.

1 Introduction

The Earth System is currently in a state of rapid warming that is unprecedented even in geological records (Pachauri et al., 2014). This change is primarily driven by the rapid increase in atmospheric concentrations of greenhouse gases (GHG) due to anthropogenic emissions since the industrial revolution (Myhre et al., 2013). Changes in natural physical and biological systems are already being observed (Rosenzweig et al., 2008), and efforts are made to determine the ‘anthropogenic impact’ on particular (extreme weather) events (Haustein et al., 2016). Nowadays, the question is not so much if, but by how much and how quickly the climate will change as a result of human interfer-



25 ence, whether this change will be smooth or bumpy (Lenton et al., 2008) and whether it will lead to dangerous anthropogenic interference with the climate (Mann, 2009).

The climate system is characterized by positive feedbacks causing instabilities, chaos and stochastic dynamics (Dijkstra, 2013) and many details of the processes determining the future behavior of the climate state are unknown. The debate on action on climate change is therefore focused on the question of *risk* and how the *probability* of dangerous climate change can be reduced. In scientific 30 and political discussions, targets on ‘allowable’ warming (in terms of change in Global Mean Surface Temperature (GMST) relative to pre-industrial conditions¹) have turned out to be salient, with the 2 K warming threshold commonly seen as a safe threshold to avoid the worst effects that might occur when positive feedbacks are unleashed (Pachauri et al., 2014). Indeed, in the Paris COP21 conference it was agreed to attempt to limit warming below 1.5 K (United Nations, 2015). It is, 35 however, questionable whether the commitments made by countries (the so-called Nationally Determined Contributions (NDCs)) are sufficient to keep temperatures below the 1.5 K and possibly even the 2.0 K target (Rogelj et al., 2016a).

A range of studies has appeared to provide insight on the safe level of cumulative emissions to stay below either the 1.5 K or 2.0 K target at a certain time in the future with a specified probability, 40 usually taken as the year 2100. Early studies made use of Earth System Models of Intermediate Complexity (EMICs) (Zickfeld et al., 2009; Huntingford et al., 2012; Steinacher et al., 2013) to obtain such estimates. Because it was found that peak warming depends on cumulative carbon emissions E_{Σ} but is independent of the emission pathway (Allen et al., 2009; Zickfeld et al., 2012), focus has been on the specification of a safe level of E_{Σ} values corresponding to a certain temperature 45 target. In more recent papers, also emulators derived from either C4MIP models (Benjamin M Sanderson, 2016) or CMIP5 (Coupled Model Intercomparison Project 5) models (Millar et al., 2017b), with specified emission scenarios, were used for this purpose. Such methodology was recently used in (Millar et al., 2017a) to argue that a post-2015 value of $E_{\Sigma} \sim 200$ GtC would limit post-2015 warming to less than 0.6°C (so meeting the 1.5 K target) with a probability of 66%.

50 In this paper we pose the following question: assume one wants to limit warming to a specific threshold in the year 2100, while accepting a certain risk tolerance of exceeding it, then, when, at the latest, does one have to start to ambitiously reduce fossil fuel emissions? The point in time when it is ‘too late’ to act in order to stay below the prescribed threshold is called (van Zalinge et al., 2017) the Point of No Return (PNR). The value of the PNR will depend on a number of quantities, such as the 55 climate sensitivity and the means available to reduce emissions. To determine estimates of the PNR, a model is required of global climate development that a) is accurate enough to give a realistic picture of the behavior of GMST under a wide range of climate change scenarios, b) is forced by fossil fuel emissions, c) is simple enough to be evaluated for a very large number of different emission and mitigation scenarios and d) provides information about risk, i.e., it cannot be purely deterministic.

¹We define pre-industrial temperature as the 1861-1880 mean temperature, in accordance with IPPC AR5.



60 The models used in van Zalinge et al. (2017) are clearly too idealized to determine adequate estimates of the PNR under different conditions. In this paper, we therefore construct a stochastic model from the CMIP5 results where many global climate models were subjected to the same forcing for a number of climate change scenarios (Taylor et al., 2012). This stochastic model is then used together with a broad range of mitigation scenarios to determine estimates of the PNR under different
65 risk tolerances.

70 If the Paris temperature targets are to be met, only a few years are left for policy makers to take action by cutting emissions (Stocker, 2013): with an emissions reduction rate of $5\% \text{ yr}^{-1}$, the 1.5 K target has become unachievable and the 2.0 K target becomes unachievable after 2017. The Stocker (2013) analysis highlights the crucial concept of the closing door or PNR of climate policy, but it is
75 deterministic. It does not take account of the possibility that these targets are not met, and does not allow for negative emissions scenarios. We here show how the considerable climate uncertainties captured by our stochastic state-space model of the carbon dynamics and temperature inertia, the degree to which policy makers are willing to take risk, and the potential of negative emissions affect the carbon budget and the date at which climate policy becomes unachievable (the PNR). The climate policy is here not defined as an exponential emission reduction as in Stocker (2013) but as a steady increase in the share of renewable energy in total energy.

2 Methods

80 We let ΔT be the annual-mean area-weighted Global Mean Surface Temperature (GMST) deviation from pre-industrial conditions of which the 1861-1880 mean is considered to be representative (Pachauri et al., 2014; Schurer et al., 2017). From the CMIP5 scenarios we use the simulations of the pre-industrial control, abrupt quadrupling of atmospheric CO₂, smooth increase of 1% CO₂ per year, and the RCP (Representative Concentration Pathways) scenarios 2.6, 4.5, 6.0 and 8.5 (Taylor et al., 2012). The data is obtained from the German Climate Computing Center (DKRZ), the ESGF Node at DKRZ, and KNMI's Climate Explorer. The CO₂ forcings (concentrations (Meinshausen et al., 2011) and emissions (van Vuuren et al., 2007; Clarke et al., 2007; Fujino et al., 2006; Riahi et al., 2007)) are obtained from the RCP Database (available at <http://tntcat.iiasa.ac.at/RcpDb>).

90 As all CMIP5 models are designed to represent similar (physical) processes but use different formulations, parametrizations, resolutions and implementations, the results from different models offer a glimpse into the (statistical) properties of future climate change, including various forms of uncertainty. We perceive each model simulation as one possible, equally likely, realization of climate change. Applying ideas and methods from statistical physics (Ragone et al., 2016), in particular Linear Response Theory (LRT), a stochastic model is constructed that represents the CMIP5 ensemble statistics of the GMST.



2.1 Linear Response Theory

95 We use only those ensemble members from CMIP5 for which the control run and at least one perturbation run are available, leading to 34 members for the abrupt (CO₂ quadrupling) and 39 for the smooth-forcing experiment. Considering those members from the RCP runs also available in the abrupt forcing run, we have 25 members for RCP2.6, 30 for RCP4.5, 19 for RCP6.0 and 29 for RCP8.5.

100 The CO₂ concentration as a function of time for the abrupt quadrupling and smooth CO₂ increase is prescribed as

$$C_{CO2,abrupt}(t) = C_0(3\theta(t) + 1) \quad (1)$$

$$C_{CO2,smooth}(t) = \begin{cases} C_0 & , \quad t \leq 0 \\ C_0 1.01^t & , \quad t > 0 \end{cases} \quad (2)$$

with time in years from the start of the forcing, pre-industrial CO₂ concentration C_0 and Heaviside function $\theta(t)$. The radiative forcing ΔF due to CO₂ relative to pre-industrial conditions is given as

$$\Delta F = \alpha_{CO2} \ln \left(\frac{C_{CO2}(t)}{C_0} \right) \quad (3)$$

with $\alpha_{CO2} = 5.35 \text{ W m}^{-2}$ (Myhre et al., 2013). With LRT, the Green's function for the temperature response is computed from the abrupt forcing case as the time derivative of the mean response (Ragone et al., 2016)

$$110 \quad G_T(t) = \frac{1}{\Delta F_{abrupt}} \frac{d}{dt} \Delta T_{abrupt} \quad (4)$$

where $\Delta F_{abrupt}(t) = \ln(4C_0/C_0) = \ln(4)$. The temperature deviation from the pre-industrial state for any forcing ΔF_{any} is then obtained, via the convolution of the Green's function, as

$$\Delta T_{any}(t) = \int_0^t G_T(t') \Delta F_{any}(t - t') dt' \quad (5)$$

Because equation (4) is exact we expect that (5) with $\Delta F_{any} = \Delta F_{abrupt}$ will exactly reproduce the abrupt CMIP5 response. In addition, for the LRT to be a useful approximation, the response has to reasonably reproduce the smooth 1% yr⁻¹ CMIP5 response with $\Delta F_{any} = \Delta F_{smooth}$. Figure 1a shows that LRT applied to the abrupt perturbation recovers perfectly – as required – the abrupt response and is well able to recover the response to a smooth forcing. The correspondence is very good for the mean response and also the variance is captured quite well. In order to apply LRT to the RCP scenarios, the radiative forcing has to be scaled up by a constant factor A as these – unlike the idealized abrupt and smooth scenarios – include non-fossil CO₂ emissions and non-CO₂ GHG emissions. The constant $A = 1.48$ was found in order to optimize the agreement of ΔT with CMIP5. The resulting reconstruction of temperatures from RCP CO₂ concentrations overlaid with CMIP5 data (Figure 1b), also gives a good agreement.



125 Beyond finding the temperature change as a result of CO₂ variations, eventually emissions E_{CO2} cause these CO₂ changes and have to be addressed explicitly. A multi-model study of many carbon models of varying complexity under different background states and forcing scenarios was recently presented (Joos et al., 2013). A fit of a three-timescale exponential with constant offset was proposed for the ensemble mean of responses to a 100 GtC emission pulse to a present-day climate of the form

130

$$G_{CO2}(t) = a_0 + \sum_{i=1}^3 a_i e^{-\frac{t}{\tau_i}} \quad (6)$$

Coefficients $a_i, i = 0 \dots 3$ and timescales $\tau_i, i = 1 \dots 3$ are determined using least-square fits on the multi-model mean. The CO₂ concentration then follows from

$$C_{CO2}(t) = \int_0^t G_{CO2}(t') E_{CO2}(t-t') dt' \quad (7)$$

135 In doing so, we use a response function that is independent of the size of the impulse, i.e. the carbon cycle reacts in the same way to pulses of all sizes other than 100 GtC. This is of course a simplification, especially as very large pulses might unleash positive feedbacks to do with the saturation of natural sinks such as the oceans (Millar et al., 2017b), but works reasonably well in the range of emissions we are primarily interested in.

The full (temperature and carbon) LRT model is summarized as

$$C_{CO2}(t) = C_{CO2,0} + \int_0^t G_{CO2}(t') E_{CO2}(t-t') dt' \quad (8a)$$

$$\Delta F_{CO2}(t) = A \alpha_{CO2} \ln(C_{CO2}(t)/C_0) \quad (8b)$$

$$\Delta T(t) = \Delta T_0 + \int_0^t G_T(t') \Delta F_{CO2}(t-t') dt' \quad (8c)$$

140 and relates fossil CO₂ emissions E_{CO2} to mean GMST perturbation ΔT with initial conditions $C_{CO2,0}$ for CO₂ and ΔT_0 for GMST perturbation. This is quite a simple model with few ‘knobs to turn’. The only really free parameter is the constant A that scales up CO₂-radiative forcing to take into account non-fossil CO₂ and non-CO₂ GHG emissions. Internally, emissions need to be converted from GtCyr⁻¹ to ppm yr⁻¹ using the respective molar masses and the mass of the Earth’s atmosphere as $E_{CO2}[\text{ppm yr}^{-1}] = \gamma E_{CO2}[\text{GtCyr}^{-1}]$ with $\gamma = 0.46969 \text{ ppm GtC}^{-1}$. In Table 1 we summarize our estimates of the model’s ten parameters.

145 In Figure 2 we show the results obtained for RCP emissions. For very high emission scenarios we underestimate CO₂ concentrations because for such emissions natural sinks saturate. However, the up-scaling of radiative forcing is quite successful, yielding a good temperature reconstruction.



150 **2.2 Stochastic State Space Model**

The model outlined above still contains a data-based temperature response function and it informs only about the *mean* CMIP5 response. However, our main motivation is to obtain new insights on the possible evolution to a ‘safe’ carbon-free, state and such paths necessarily depend strongly on the variance of the climate and on the risk one is willing to take. This variance in temperature is
 155 quite substantial, as is evident from Figure 1b. Therefore we translate our response function model to a state-space model and incorporate the variance via suitable stochastic terms.

The response function G_T from the 140-year abrupt quadrupling ensemble is well approximated by

$$G_T(t) = \sum_{i=0}^2 b_i e^{-\frac{t}{\tau_{bi}}} \quad (9)$$

Although $\tau_{b0} \rightarrow \infty$, we require a finite τ_{b0} for temperatures to stabilize at some level. Hence, we choose a long time scale $\tau_{b0} = 400$ yr that cannot really be determined from the 140 yr abrupt forcing (CMIP5) runs. By writing

$$C = C_P + \sum_{i=1}^3 C_i \quad (10a)$$

$$\Delta T = \sum_{i=0}^2 \Delta T_i \quad (10b)$$

160 the LRT model can be transformed into the 7-dimensional Stochastic State Space Model (SSSM) shown in Table 2 with parameters in Table 3. Initial conditions are obtained by running the noise-free model forward from pre-industrial conditions ($C_P = C_0$ and $C_i = \Delta T_i = 0, i = 1, 2, 3$) to present-day, driven by historical emissions². As these temperatures are now given relative to the start of emissions, i.e. 1765, we add the 1961-1990 model mean to the HadCRUT4 dataset to get observed
 165 temperature deviation relative to 1765, and compute ΔT relative to 1861-1880 by adding the 1861-1880 mean of this deviation time series.

The major benefit of this formulation is that we can include stochasticity. We introduce additive noise to the carbon model such that the standard deviation of the model response to an emission pulse as reported by (Joos et al., 2013) is recovered. For the temperature model we introduce (small) additive noise to recover the (small) CMIP5 control run standard deviation. In the CMIP5 RCP runs the ensemble variance increases with rising ensemble mean. This calls for the introduction of (substantial) multiplicative noise, which we introduce in ΔT_2 , letting these random fluctuations decay over an 8-year timescale. The magnitude of these fluctuations is (especially at high temperatures) likely to be unrealistic when looking at individual time series. However, the focus here is on ensemble
 175 statistics.

²these are the fossil fuel and cement production emissions from (Le Quéré et al., 2016), accessed 28th March, 2017



2.3 Transition Pathways

The SSSM described in the previous section is forced with fossil CO₂ emissions. We assume that, in the absence of any mitigation actions, emissions increase from their initial value E_0 at an exponential rate g due to economic and population growth. Political decisions cause emissions to decrease from 180 starting year t_s onward as fossil energy generation is replaced by non-GHG producing forms such as wind, solar and water (mitigation m) and by an increasing share of fossil energy sources the emissions of which are not released but captured and stored away by Carbon Capture and Storage (abatement a). In addition, negative emission technologies E_{neg} may be employed that lead to a net reduction in atmospheric CO₂ concentration. We model this in a very simple way by letting both 185 mitigation and abatement increase linearly until emissions are brought to zero:

$$m(t) = \begin{cases} m_0 & t \leq t_s \\ \min(m_0 + m_1(t - t_s), 1) & t > t_s \end{cases} \quad (11a)$$

$$a(t) = \begin{cases} a_0 & t \leq t_s \\ \min(a_0 + a_1(t - t_s), 1) & t > t_s \end{cases} \quad (11b)$$

$$E(t) = E_0 e^{gt} (1 - a(t))(1 - m(t)) - E_{neg}(t) \quad (11c)$$

with constants m_0, a_0 giving the mitigation and abatement rates at the start of the scenario and m_1 190 the incremental year-to-year increase. The simplified model (11) is very well able (not shown) to reproduce the IAM pathways from that fulfil the NDCs until 2030 and afterwards reach the 2 K target with a 50-66% probability (Rogelj et al., 2016a). These pathways are exemplary for those that continue on the low-commitment path for a while, followed by strong and decisive action.

2.4 Point of No Return

195 With the emission scenarios and the SSSM - returning CO₂ concentrations and GMST for any such scenario - one can now address the issue of transitioning from the present-day (year 2015) to a carbon-free era such as to avoid catastrophic climate change. We need to take into account both the *target* threshold and the *risk* one is willing to take to exceed it. The maximum amount of cumulative CO₂ emissions that allows reaching the 1.5 and 2 K targets, as a function of the risk tolerance, is 200 called the Safe Carbon Budget (SCB). It is well established in the literature (Meinshausen et al., 2009; Zickfeld et al., 2009) but does not contain information on how these emissions are spread in time. This is where the Point of No Return (PNR) comes in: The PNR is the point in time where starting mitigating action is insufficient to stay below a specified target with a chosen risk tolerance.

Concretely, let the temperature target ΔT_{max} be the maximum allowable warming and denote the 205 parameter β as the probability of staying below a given target (a measure of the risk tolerance). For example the case $\Delta T_{max} = 2$ K and $\beta = 0.9$ corresponds to a 90% probability of staying below 2 K



warming, i.e. 90 of 100 realizations of the SSSM, started in 2015 and integrated until 2100, do not exceed 2 K in the year 2100.

Then, in the context of (11), the PNR is the earliest t_s that does not result in reaching the defined
210 ‘Safe State’ (van Zalinge et al., 2017) in terms of ΔT_{max} and β . It is determined from the probability distribution $p(\Delta T_{2100})$ of GMST in 2100. Both SCB and PNR depend on temperature target, climate uncertainties and risk tolerance, but the PNR also depends on the aggressiveness of the climate action considered feasible (here given by the value of m_1). This makes the PNR such an interesting quantity, since the SCB does not depend on the time path of emission reductions. Clearly there is a
215 close connection between the PNR and the SCB. Indeed, one could define a PNR also in terms of the ability to reach the SCB. The one-to-one relation between cumulative emissions and warming gives the PNR in ‘carbon space’. Its location in time, however, depends crucially on how fast a transition to a carbon-neutral economy is feasible.

Since it is now recognized that negative emissions may be essential in meeting temperature targets,
220 we include this possibility into the PNR computation. From the IAM scenarios that Rogelj et al. (2016a) found to fulfill NDCs until 2030 and stay below 2 K with 50-66% probability, we obtain a family of negative emission pathways (Figure 3) out of which we pick a ‘moderate’ (orange) and a ‘strong’ (red) pathway.

3 Results

225 To demonstrate the quality of the SSSM we initialise it at pre-industrial conditions, run it forward and compare the results with those of CMIP5 models. The SSSM is well able to reproduce the CMIP5 model behavior under the different RCP scenarios (Figure 4, shown for RCP2.6 and 4.5). As these scenarios are very different in terms of rate of change and total cumulative emissions this is not a trivial finding. It is actually remarkable that the SSSM, which is based on a limited amount of
230 CMIP5 model ensemble members, performs so well. As an example, the RCP2.6 scenario contains substantial negative emissions, responsible for the downward trend in GMST, which our SSSM correctly reproduces. The mean response for RCP8.5 is slightly underestimated (not shown) because the uncertainty in the carbon cycle plays a rather minor role compared to that in the temperature model. In addition, for such large emission reductions positive feedback loops set in from which our
235 SSSM abstracts. The temperature perturbation ΔT is very closely log-normally distributed while for weak forcing scenarios (e.g., RCP2.6 and RCP4.5) the distribution is approximately Gaussian. The CO₂ concentration is found to be Gaussian distributed for all RCP scenarios. These findings (log-normal temperature and Gaussian CO₂ concentration) result from the multiplicative and additive noise in temperature and carbon components of the SSSM, respectively.

240 To determine the SCB, 6000 emission reduction strategies (with $E_{neg}(t) = 0$) were generated and, using the SSSM, an 8000-member ensemble for each of these emission scenarios starting in 2015



was integrated. Emission scenarios are generated from (11) by letting $a(t) = 0$, a uniform $m_0 \in [0, 0.7]$ and m_1 drawn from a beta distribution (with distribution function $p(m) = \frac{1}{B(\alpha, \delta)} m^\alpha (1-m)^{\delta-1}$, where $B(\alpha, \delta)$ is the beta function; parameters are chosen as $\alpha = 1.2, \delta = 3$), with the 245 [0,1] interval scaled such that $m = 1$ latest in 2080.

The temperature anomaly in 2100 (ΔT_{2100}) as a function of cumulative CO₂ emissions E_Σ is shown in Figure 5. The same calculation is also shown for the deterministic case without climate uncertainty (no noise in the SSSM). In Figure 5, the SCB is given by the point on the E_Σ -axis where the (colored) line corresponding to a chosen risk tolerance crosses the (horizontal) line corresponding 250 to a chosen temperature threshold ΔT_{max} . The curves $\Delta T_{2100} = f(E_\Sigma)$ (Figure 5) are very well described by expressions of the type

$$f(E_\Sigma) = a \ln \left(\frac{E_\Sigma}{b} + 1 \right) + c \quad (12)$$

with suitable coefficients a, b and c , each depending on the tolerance β . For the range of emissions considered here, a linear fit would be reasonable (Allen et al., 2009). However, our expression also 255 works for cumulative emissions in the range of business as usual (when fitting parameters on suitable emission trajectories). From Figure 5 we easily find the SCB for any combination of ΔT_{max} and β , as shown in Table 4.

Allowable emissions are drastically reduced when enforcing the target with a higher probability (following the horizontal lines from right to left in Figure 5). These results show in particular the 260 challenges posed by the 1.5 K compared to the 2 K target. The sensitivity of the SCB to the relevant model parameters is shown in the Appendix and the values are robust. From IPCC-AR5 (IPPC, 2013) we find cumulative emissions post-2015 of 377 GtC to 517 GtC in order to ‘likely’ stay below 2 K while we find an SCB of 424 GtC for $\Delta T_{max} = 2\text{K}, \beta = 0.67$ which lies in the same range. Like Millar et al. (2017a) we find approximately 200 GtC to stay below 2 K with $\beta = 0.67$.

265 To determine the PNR, we resort to three illustrative choices to model the abatement and mitigation rates with $E_{neg}(t) = 0$. Following (11) we construct Fast Mitigation (FM) and Moderate Mitigation (MM) scenarios with $m_1 = 0.05$ and 0.02 , respectively. In addition, in an Extreme Mitigation (EM) scenario $m = 1$ can be reached instantaneously. This corresponds to the most extreme physically possible scenario and serves as an upper bound. When varying t_s to find the PNR for 270 the three scenarios, we always keep $m_0 = 0.14$ and $a_0 = 0$ at 2015 values (World Energy Council, 2016).

As an example, $t_s = 2025$ leads to total cumulative emissions from 2015 onward of 109, 183 and 275 335 GtC for the mitigation scenarios EM, FM and MM, respectively. Note that while MM is the most modest scenario, it is actually quite ambitious, considering that with $m = 0.1355$ in 2005 and $m = 0.14$ in 2015 (World Energy Council, 2016) the current year-to-year increases in the share of renewable energies are very small.

Figure 6 shows the probabilities for staying below the 1.5 and 2.0 K thresholds in 2100 as function of t_s for different policies, including FM ($m_1 = 0.05$) and MM ($m_1 = 0.02$), while the EM policy



bounds the unachievable region. It is clear that this region is larger for the 1.5 than for the 2.0
280 degree target, and shrinks when including negative emissions. From the plot we can directly see the
consequences of delaying action until a given year. For example, if policy makers should choose to
implement the MM strategy only in 2040, the chances of reaching the 1.5 (2.0) degree target are
only 2% (47%). We conclude that the remaining ‘window of action’ may be small, but a window
still exists for both targets. For example, the 2 K target is reached with a probability of 67% even
285 when starting MM is delayed until 2035. However, reaching the 1.5 K target appears unlikely as
MM would be required to start in 2018 for a probability of 67%. When requiring a high (≥ 0.9)
probability, it is impossible to reach with the MM scenario. The PNR for the different targets and
probabilities is given in Table 5. The robustness of these PNR values is shown in the Appendix.

We also see from Figure 6 and Table 7 that the inclusion of negative emissions delays the PNR by
290 6-10 years (see Table 7), which may be very valuable especially for ambitious targets. For example,
when including ‘strong’ negative emissions one can reach 1.5 K with a probability of up to 66% in
the MM scenario when acting before 2026, 8 years later than without. The PNR varies substantially
for slightly different temperature targets. This also illustrates the importance of the temperature
baseline relative to which ΔT is defined. This has been found previously (Schurer et al., 2017), and
295 we find (not shown) that switching to an 18th century baseline can move the PNR earlier by up to
10 years.

It is clear that an energy transition more ambitious than RCP2.6 is required to stay below 1.5 K
with some acceptable probability, and whether that is feasible is doubtful. For all other RCP scenarios,
exceeding 2 K is very likely in this century (Figure 7).

300 4 Summary, Discussion and Conclusions

We have developed a novel stochastic state space model (SSSM) to accurately capture the basic
statistical properties (mean and variance) of the CMIP5 RCP ensemble, allowing us to study warming
probabilities as function of emissions. It represents an alternative to the approach that contains
305 stochasticity in the parameters rather than the state. Although the model is highly idealized, it cap-
tures simulations of both temperature and carbon responses to RCP emission scenarios quite well.

A weakness of the SSSM is the simulation of temperature trajectories beyond 2100 and for high
emission scenarios. The large multiplicative noise factor leads – especially at high mean warmings –
to immensely volatile trajectories that in all likelihood are not physical (on the individual level, the
distribution is still well-behaved). It might be a worthy endeavour to investigate how this could be
310 improved. Another weakness in the carbon component part of the SSSM is that the real carbon cycle
is not pulse-independent. Hence, using a single constant response function has inherent problems, in
particular when running very high-emission scenarios. This is because the efficiency of the natural
carbon sinks to the ocean and land reservoirs is a function both of temperature and the reservoir



sizes. The SSSM has therefore slight problems reproducing CO₂ concentration pathways (Figure 315 2), a price we accept to pay as we focus on the CMIP5 temperature reproduction. Taking account of non-CO₂ emissions more fully beyond our simple scaling and avoiding temporary overshoots of the temperature caps would reduce the carbon budgets (Rogelj et al., 2016b) and thus lead to earlier PNRs than given here. Therefore the values might be a little too optimistic.

In Millar et al. (2017b), the authors draw a different conclusion from studying a similar problem. 320 They introduce in their FAIR model response functions that dynamically adjust parameters based on warming to represent sink saturation. Consequently, their model gives much better results in terms of CO₂ concentrations. It would be an interesting lead for future research to conduct our analysis here (in terms of SCB and PNR) with other simple models (such as FAIR or MAGICC) to discover 325 similarities and differences. However, only rather low-emission scenarios are consistent with the 1.5 or 2 K targets, so we do not expect this to play a major role, and indeed our carbon budgets are very similar to Millar et al. (2017a).

The concept of a Point of No Return introduces a novel perspective into the discussion of carbon budgets that is often centered on the question of when the remaining budget will have ‘run out’ 330 at current emissions. In contrast, the PNR concept recognizes the fact that emissions will not stay constant and can decay faster or slower depending on political decisions. With these caveats in mind, we conclude that, first, the PNR is still relatively far away for the 2.0 K target: with the MM scenario and $\beta = 67\%$ we have 17 years left to start. When allowing to set all emissions to zero 335 instantaneously, the PNR is even delayed to the 2050s. Considering the slow speed of large-scale political and economic transformations, decisive action is still warranted, as the MM scenario is a large change compared to current rates. Second, the PNR is very close or passed for the 1.5 K target. 340 Here more radical action is required – 9 years remain to start the FM policy to avoid 1.5 K with a 67% chance, and strong negative emissions gives us 8 years under the MM policy.

Third, we can clearly show the effects of changing ΔT_{max} , β and the mitigation scenario. Switching 345 from 1.5 to 2 K buys an additional ≈ 16 years. Allowing a one-third, instead of one-tenth exceedance risk, buys an additional 7-9 years. Allowing for the more aggressive FM policy instead of MM buys an additional 10 years. This allows to assess trade-offs, for example between tolerating higher exceedance risks and implementing more radical policies. Fourth, negative emissions can offer a brief respite but only delay the PNR by a few years, not taking into account the possible decrease in effectiveness of these measures in the long term (Tokarska and Zickfeld, 2015).

345 We have shown the constraints put on future emissions by restricting GMST increase below 1.5 and 2 K, respectively, and the crucial importance of the safety probability. Further (scientific and political) debate is essential on what are the right values for both temperature threshold and probability. Our findings are sobering in light of the bold ambition in the Paris agreement, and add to the sense of urgency to act quickly before the PNR has been crossed.



350 *Acknowledgements.* We thank the focus area 'Foundations of Complex Systems' of Utrecht University for providing the finances for the visit of F. van der Ploeg to Utrecht in 2016. HAD acknowledges support by the Netherlands Earth System Science Centre (NESSC), financially supported by the Ministry of Education, Culture and Science (OCW), Grant no. 024.002.001.



References

355 Allen, M. R., Frame, D. J., Huntingford, C., Jones, C. D., Lowe, J. A., Meinshausen, M., and Meinshausen, N.: Warming caused by cumulative carbon emissions towards the trillionth tonne, *Nature*, 458, 1163–1166, doi:10.1038/nature08019, 2009.

Benjamin M Sanderson, B. C. O. C. T.: What would it take to achieve the Paris temperature targets?, *Geophysical Research Letters*, pp. 1–10, 2016.

360 Clarke, L. E., Edmonds, J. A., Jacoby, H. D., Pitcher, H. M., Reilly, J. M., and Richels, R. G.: Scenarios of Greenhouse Gas Emissions and Atmospheric Concentrations Synthesis, Tech. rep., Department of Energy, Office of Biological & Environmental Research, Washington, D.C., 2007.

Dijkstra, H. A.: Nonlinear Climate Dynamics, Cambridge University Press, Cambridge, doi:10.1017/CBO9781139034135, 2013.

365 Fujino, J., Nair, R., Kainuma, M., Masui, T., and Matsuoka, Y.: Multi-gas Mitigation Analysis on Stabilization Scenarios Using AIM Global Model, *The Energy Journal*, SI 2006, 343–354, doi:10.5547/ISSN0195-6574-EJ-VolSI2006-NoSI3-17, 2006.

Haustein, K., Otto, F. E. L., Uhe, P., Schaller, N., Allen, M. R., Hermanson, L., Christidis, N., McLean, P., and Cullen, H.: Real-time extreme weather event attribution with forecast seasonal SSTs, *Environmental Research Letters*, 11, 064 006, doi:10.1088/1748-9326/11/6/064006, 2016.

370 Huntingford, C., Lowe, J. A., Gohar, L. K., Bowerman, N. H. A., Allen, M. R., Raper, S. C. B., and Smith, S. M.: The link between a global 2°C warming threshold and emissions in years 2020, 2050 and beyond, *PNAS*, 7, 014 039–9, 2012.

IPPC: Climate Change 2013: The Physical Science Basis. Contribution of Working Group I to the Fifth Assessment Report of the Intergovernmental Panel on Climate Change, Cambridge University Press, Cambridge, UK and New York, NY, USA, 2013.

375 Joos, F., Roth, R., Fuglestvedt, J. S., Peters, G. P., Enting, I. G., von Bloh, W., Brovkin, V., Burke, E. J., Eby, M., Edwards, N. R., Friedrich, T., Frölicher, T. L., Halloran, P. R., Holden, P. B., Jones, C., Kleinen, T., Mackenzie, F. T., Matsumoto, K., Meinshausen, M., Plattner, G.-K., Reisinger, A., Segschneider, J., Shaffer, G., Steinacher, M., Strassmann, K., Tanaka, K., Timmermann, A., and Weaver, A. J.: Carbon dioxide and climate impulse response functions for the computation of greenhouse gas metrics: a multi-model analysis, *Atmospheric Chemistry and Physics*, 13, 2793–2825, doi:10.5194/acp-13-2793-2013, 2013.

Le Quéré, C., Andrew, R. M., Canadell, J. G., Sitch, S., Korsbakken, J. I., Peters, G. P., Manning, A. C., Boden, T. A., Tans, P. P., Houghton, R. A., Keeling, R. F., Alin, S., Andrews, O. D., Anthoni, P., Barbero, L., Bopp, L., Chevallier, F., Chini, L. P., Ciais, P., Currie, K., Delire, C., Doney, S. C., Friedlingstein, P., Gkritzalis, T., Harris, I., Hauck, J., Haverd, V., Hoppema, M., Klein Goldewijk, K., Jain, A. K., Kato, E., Körtzinger, A., Landschützer, P., Lefèvre, N., Lenton, A., Lienert, S., Lombardozzi, D., Melton, J. R., Metzl, N., Millero, F., Monteiro, P. M. S., Munro, D. R., Nabel, J. E. M. S., Nakaoka, S.-i., O'Brien, K., Olsen, A., Omar, A. M., Ono, T., Pierrot, D., Poulter, B., Rödenbeck, C., Salisbury, J., Schuster, U., Schwinger, J., Séférian, R., Skjelvan, I., Stocker, B. D., Sutton, A. J., Takahashi, T., Tian, H., Tilbrook, B., van der Laan-Luijkx, I. T., van der Werf, G. R., Viovy, N., Walker, A. P., Wiltshire, A. J., and Zaehle, S.: Global Carbon Budget 2016, *Earth System Science Data*, 8, 605–649, doi:10.5194/essd-8-605-2016, 2016.



1 Lenton, T. M., Held, H., Kriegler, E., Hall, J. W., Lucht, W., Rahmstorf, S., and Schellnhuber, H. J.: Tipping
elements in the Earth's climate system, *Proceedings of the National Academy of Sciences*, 105, 1786–1793,
395 doi:10.1073/pnas.0705414105, 2008.

2 Mann, M. E.: Defining dangerous anthropogenic interference., *Proceedings of the National Academy of Sciences of the United States of America*, 106, 4065–4066, doi:10.1073/pnas.0901303106, 2009.

3 Meinshausen, M., Meinshausen, N., Hare, W., Raper, S. C. B., Frieler, K., Knutti, R., Frame, D. J., and Allen,
400 M. R.: Greenhouse-gas emission targets for limiting global warming to 2 °C, *Nature*, 458, 1158–1162,
doi:10.1038/nature08017, 2009.

4 Meinshausen, M., Smith, S. J., Calvin, K., Daniel, J. S., Kainuma, M. L. T., Lamarque, J.-F., Matsumoto, K.,
Montzka, S. A., Raper, S. C. B., Riahi, K., Thomson, A., Velders, G. J. M., and van Vuuren, D. P.: The RCP
greenhouse gas concentrations and their extensions from 1765 to 2300, *Climatic Change*, 109, 213–241,
doi:10.1007/s10584-011-0156-z, 2011.

5 Millar, R. J., Fuglestvedt, J. S., Friedlingstein, P., Rogelj, J., Grubb, M. J., Matthews, H. D., Skeie, R. B., Forster,
P. M., Frame, D. J., and Allen, M. R.: Emission budgets and pathways consistent with limiting warming to
1.5°C, *Nature Geosci*, 10, 741–747, 2017a.

6 Millar, R. J., Nicholls, Z. R., Friedlingstein, P., and Allen, M. R.: A modified impulse-response representation of
the global near-surface air temperature and atmospheric concentration response to carbon dioxide emissions,
410 *Atmospheric Chemistry and Physics*, 17, 7213–7228, doi:10.5194/acp-17-7213-2017, 2017b.

7 Myhre, G., Shindell, D., Bréon, F.-M., Collins, W., Fuglestvedt, J., Huang, J., Koch, D., Lamarque, J.-F., Lee,
D., Mendoza, B., Nakajima, T., Robock, A., Stephens, T., Takemura, T., and Zhang, H.: Anthropogenic
and Natural Radiative Forcing, in: *Climate Change 2013 - The Physical Science Basis*, edited by Inter-
governmental Panel on Climate Change, chap. 8, pp. 659–740, Cambridge University Press, Cambridge,
415 doi:10.1017/CBO9781107415324.018, 2013.

8 Pachauri, R. K., Allen, M. R., Barros, V. R., Broome, J., Cramer, W., Christ, R., Church, J. A., Clarke, L.,
Dahe, Q., Dasgupta, P., Dubash, N. K., Edenhofer, O., Elgizouli, I., Field, C. B., Forster, P., Friedlingstein,
P., Fuglestvedt, J., Gomez-Echeverri, L., Hallegatte, S., Hegerl, G., Howden, M., Jiang, K., Cisneros, B. J.,
Kattsov, V., Lee, H., Mach, K. J., Marotzke, J., Mastrandrea, M. D., Meyer, L., Minx, J., Mulugetta, Y.,
420 O'Brien, K., Oppenheimer, M., Pereira, J. J., Pichs-Madruga, R., Plattner, G.-K., Pörtner, H.-O., Power,
S. B., Preston, B., Ravindranath, N. H., Reisinger, A., Riahi, K., Rusticucci, M., Scholes, R., Seyboth, K.,
Sokona, Y., Stavins, R., Stocker, T. F., Tschakert, P., van Vuuren, D., and van Ypersele, J.-P.: *Climate Change
2014: Synthesis Report. Contribution of Working Groups I, II and III to the Fifth Assessment Report of the
Intergovernmental Panel on Climate Change*, IPCC, Geneva, Switzerland, 2014.

425 9 Ragone, F., Lucarini, V., and Lunkeit, F.: A new framework for climate sensitivity and prediction: a modelling
perspective, *Climate Dynamics*, 46, 1459–1471, doi:10.1007/s00382-015-2657-3, 2016.

10 Riahi, K., Grubler, A., and Nakicenovic, N.: Scenarios of long-term socio-economic and environmental
development under climate stabilization, *Technological Forecasting and Social Change*, 74, 887–935,
doi:10.1016/j.techfore.2006.05.026, 2007.

11 Rogelj, J., den Elzen, M., Höhne, N., Fransen, T., Fekete, H., Winkler, H., Schaeffer, R., Sha, F., Riahi, K.,
12 and Meinshausen, M.: Paris Agreement climate proposals need a boost to keep warming well below 2°C ,
Nature, 534, 631–639, doi:10.1038/nature18307, 2016a.



Rogelj, J., Schaeffer, M., Friedlingstein, P., Gillett, N. P., van Vuuren, D. P., Riahi, K., Allen, M., and Knutti, R.: Differences between carbon budget estimates unravelled, *Nature Climate Change*, 6, 245–252, 435 doi:10.1038/nclimate2868, 2016b.

Rosenzweig, C., Karoly, D., Vicarelli, M., Neofotis, P., Wu, Q., Casassa, G., Menzel, A., Root, T. L., Estrella, N., Seguin, B., Tryjanowski, P., Liu, C., Rawlins, S., and Imeson, A.: Attributing physical and biological impacts to anthropogenic climate change, *Nature*, 453, 353–357, doi:10.1038/nature06937, 2008.

Schurer, A. P., Mann, M. E., Hawkins, E., Tett, S. F. B., and Hegerl, G. C.: Importance of the pre-industrial 440 baseline for likelihood of exceeding Paris goals, *Nature Climate Change*, 7, 563–567, 2017.

Steinacher, M., Joos, F., and Stocker, T. F.: Allowable carbon emissions lowered by multiple climate targets, *Nature*, 499, 197–201, 2013.

Stocker, T. F.: The Closing Door of Climate Targets, *Science*, 339, 280–282, doi:10.1126/science.1232468, 2013.

445 Taylor, K. E., Stouffer, R. J., and Meehl, G. A.: An Overview of CMIP5 and the Experiment Design, *Bulletin of the American Meteorological Society*, 93, 485–498, doi:10.1175/BAMS-D-11-00094.1, 2012.

Tokarska, K. B. and Zickfeld, K.: The effectiveness of net negative carbon dioxide emissions in reversing anthropogenic climate change, *PNAS*, 10, 1–11, 2015.

United Nations: Adoption of the Paris Agreement, Framework Convention on Climate Change, 21st Conference 450 of the Parties, Paris, 2015.

van Vuuren, D. P., den Elzen, M. G. J., Lucas, P. L., Eickhout, B., Strengers, B. J., van Ruijven, B., Wonink, S., and van Houdt, R.: Stabilizing greenhouse gas concentrations at low levels: an assessment of reduction strategies and costs, *Climatic Change*, 81, 119–159, doi:10.1007/s10584-006-9172-9, 2007.

van Zalinge, B. C., Feng, Q. Y., Aengenheyster, M., and Dijkstra, H. A.: On determining the Point of no Return 455 in Climate Change, *Earth System Dynamics*, 8, 707–717, doi:10.5194/esd-2016-40, 2017.

World Energy Council: *World Energy Resources 2016*, Tech. rep., World Energy Council, London, 2016.

Zickfeld, K., Eby, M., Matthews, H. D., and Weaver, A. J.: Setting cumulative emissions targets to reduce the risk of dangerous climate change, *Proceedings of the National Academy of Sciences*, 106, 16 129–16 134, doi:10.1073/pnas.0805800106, 2009.

460 Zickfeld, K., Arora, V. K., and Gillett, N. P.: Is the climate response to CO₂ emissions path dependent?, *Geophysical Research Letters*, 39, doi:10.1029/2011GL050205, 2012.

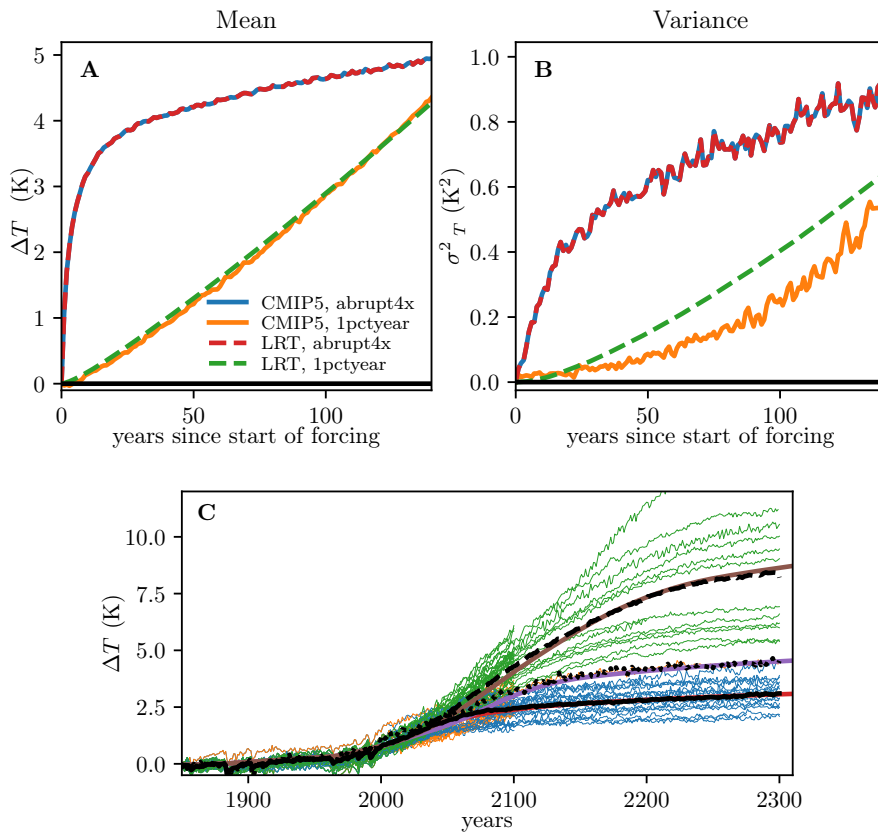


Figure 1. Ensemble mean (**A**) and variance (**B**) of temperature response from CMIP5 (solid) and LRT reproduction (dashed). Year 0 gives the start of the perturbation. (**C**) Reconstruction of RCP temperature evolution from concentration pathways using CO₂ only. Blue, orange and green lines gives CMIP5 data for RCP4.5, RCP6.0 and RCP8.5, respectively, with the ensemble mean given in black solid (RCP4.5), dotted (RCP6.0) and dashed (RCP8.5) black. Reconstruction using CO₂ radiative forcing in red (RCP4.5), purple (RCP6.0) and brown (RCP8.5).

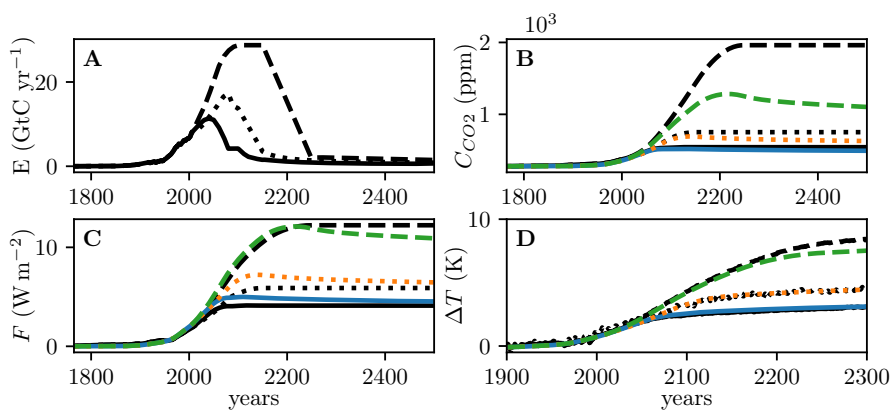


Figure 2. Reconstruction of RCP results using the Response Function Model. In all panels, solid lines refer to RCP4.5, dotted to RCP6.0 and dashed lines to RCP8.5. Black lines show RCP data while colors (blue: RCP4.5, orange: RCP6.0, green: RCP8.5) give our reconstruction. **(A):** Fossil CO₂ emissions. **(B):** CO₂ concentrations from RCP and reconstructed using G_{CO_2} . **(C):** Total anthropogenic radiative forcing (black) and radiative forcing from CO₂ only (red) (both from RCP) and reconstructed forcing using the relations above. **(D):** Temperature perturbation from CMIP5 RCP (ensemble mean) and the our reconstruction.

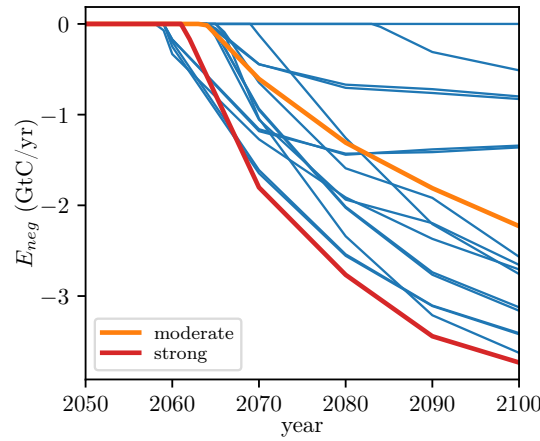


Figure 3. Negative Emissions from IAM scenarios (Rogelj et al., 2016a), with two sample pathways marked.

C_0 (ppm)	a_0	a_1	a_2	a_3
278	0.2173	0.2240	0.2824	0.2763
A	α (W m^{-2})	τ_1	τ_2	τ_3
1.48	5.35	394.4	36.54	4.304

Table 1. Response Function Model Parameters. All timescales τ_i are in years and the carbon model amplitudes a_i are dimensionless for E in ppm yr^{-1} .

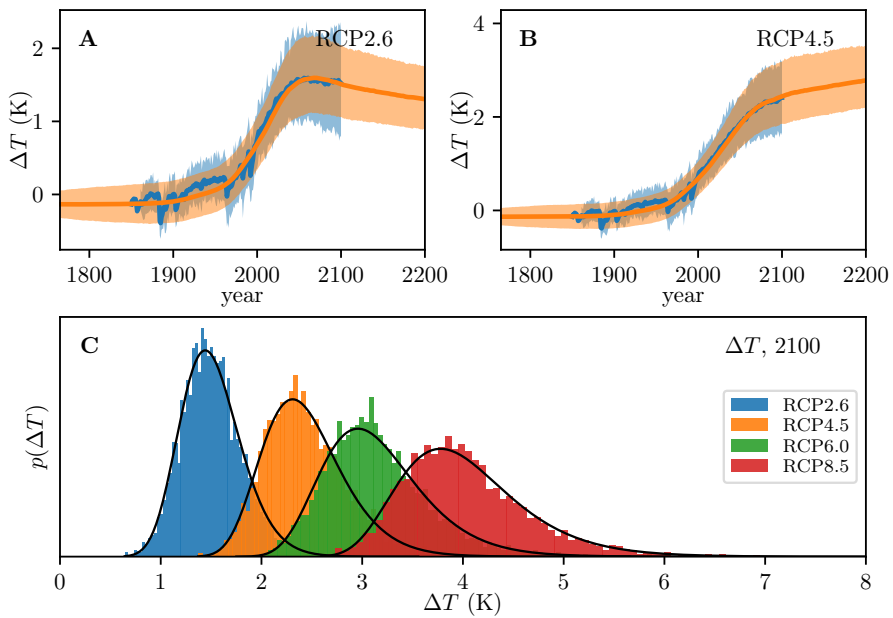


Figure 4. Stochastic State Space Model applied to RCP scenarios. **(A,B):** Ensemble mean and 5th, 95th percentile envelopes of CMIP5 RCPs (blue) and stochastic model (orange). **(C):** Probability density functions for ΔT in 2100 based on 5000 ensemble members, and driven by forcing from RCP2.6 (blue), RCP4.5 (orange), RCP6.0 (green) and RCP8.5 (red). In black are fitted lognormal distributions.

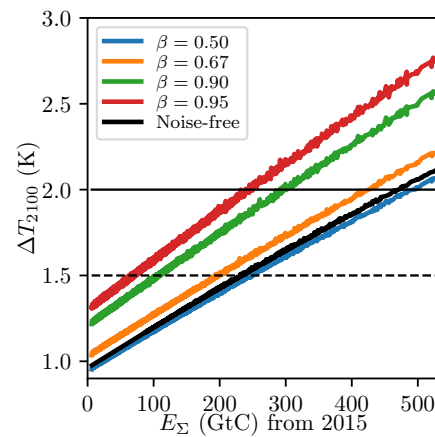


Figure 5. The Safe Carbon Budget, ΔT_{max} in 2100 such that $p(\Delta T_{2100} \leq \Delta T_{max}) = \beta$ as a function of cumulative emissions for different β . The black curve gives the deterministic results with noise terms in the stochastic model set to zero.

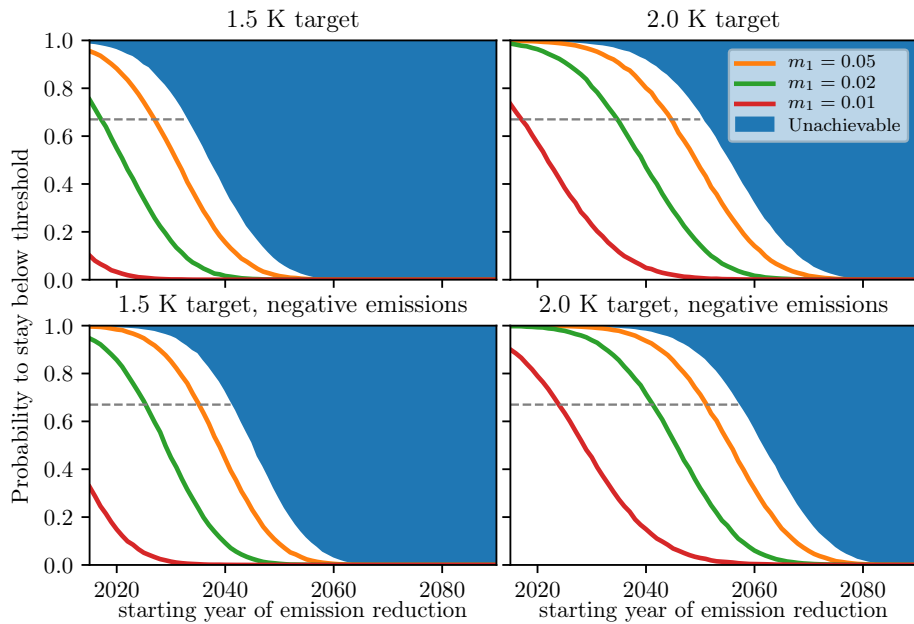


Figure 6. The Point of No Return. Probability of staying below the 1.5 K (left) or 2.0 K (right) threshold when starting emission reductions in a given year, for different policies, without (top) and with (bottom) strong negative emissions. The Point of No Return for a given policy is given by the point in time where the probability drops below a chosen threshold. The default threshold of two-thirds is dashed. The unachievable region is bounded by the extreme mitigation scenario.

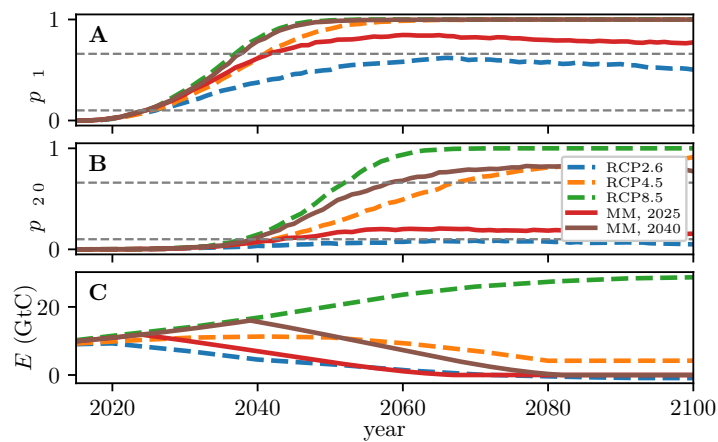


Figure 7. (A,B): Instantaneous probability to exceed 1.5 K (A) and 2.0 K (B) for different emission scenarios. RCP scenarios are shown as dashed lines while solid lines give MM scenario results starting in 2025 (red) and 2040 (brown). Dashed horizontal lines give $p = 0.1$ and 0.67 , respectively. (C): Fossil fuel emissions in GtC for the same scenarios.



$$\begin{aligned}
 dC_P &= a_0 E dt & \Delta F &= A \alpha \ln(C/C_0) \\
 dC_1 &= (a_1 E - \frac{1}{\tau_1} C_1) dt & d\Delta T_0 &= (b_0 \Delta F - \frac{1}{\tau_{b0}} \Delta T_0) dt + \sigma_{T0} dW_t \\
 dC_2 &= (a_2 E - \frac{1}{\tau_2} C_2) dt + \sigma_{C2} dW_t & d\Delta T_1 &= (b_1 \Delta F - \frac{1}{\tau_{b1}} \Delta T_1) dt \\
 dC_3 &= (a_3 E - \frac{1}{\tau_3} C_3) dt & d\Delta T_2 &= (b_2 \Delta F - \frac{1}{\tau_{b2}} \Delta T_2) dt + \sigma_{T2} \Delta T_2 dW_t \\
 C &= C_P + \sum_{i=1}^3 C_i & \Delta T &= \sum_{i=0}^2 \Delta T_i
 \end{aligned}$$

Table 2. Stochastic State Space Model. Carbon model on left, temperature model on the right.

a_0	a_1	a_2	a_3	τ_1	τ_2	τ_3
0.2173	0.2240	0.2824	0.2763	394.4	36.54	4.304
C_0 (ppm)	b_0	b_1	b_2	τ_{b0}	τ_{b1}	
278	0.00115176	0.10967972	0.03361102	400	1.42706247	
A	α (W m^{-2})	σ_{C2} (ppm/yr $^{1/2}$)	σ_{T0} (K/yr $^{1/2}$)	σ_{T2} (yr $^{-1/2}$)	τ_{b2}	
1.48	5.35	0.65	0.015	0.13	8.02118539	

Table 3. Stochastic State Space Model Parameters. All timescales are in years, the carbon model amplitudes a_i are dimensionless for E in ppm yr $^{-1}$, the temperature model amplitudes b_i are in K $\text{W}^{-1} \text{m}^2 \text{yr}^{-1}$.



β	0.5	0.67	0.9	0.95	Noise-free
$T_{max} = 1.5\text{K}$	247	198	107	69	233
$T_{max} = 2.0\text{K}$	492	424	298	245	469

Table 4. Safe Carbon Budget (in GtC since 2015) as function of threshold and safety probability β .

	β	0.5	0.67	0.9	0.95	noise-free
EM	$T_{max} = 1.5\text{K}$	2038	2034	2026	2022	2037
	$T_{max} = 2.0\text{K}$	2056	2051	2042	2038	2055
FM	$T_{max} = 1.5\text{K}$	2032	2027	2020	2016	2030
	$T_{max} = 2.0\text{K}$	2050	2045	2036	2032	2048
MM	$T_{max} = 1.5\text{K}$	2022	2018	—	—	2021
	$T_{max} = 2.0\text{K}$	2040	2035	2026	2022	2038

Table 5. Point of No Return as function of threshold and safety probability β without negative emissions.

	β	0.5	0.67	0.9	0.95	noise-free
EM	$T_{max} = 1.5\text{K}$	2046	2042	2035	2032	2045
	$T_{max} = 2.0\text{K}$	2062	2058	2049	2046	2061
FM	$T_{max} = 1.5\text{K}$	2039	2036	2028	2025	2038
	$T_{max} = 2.0\text{K}$	2056	2052	2043	2039	2055
MM	$T_{max} = 1.5\text{K}$	2029	2026	2019	—	2029
	$T_{max} = 2.0\text{K}$	2046	2042	2033	2030	2045

Table 6. Point of No Return as function of threshold and safety probability β with strong negative emissions.

	β	0.5	0.67	0.9	0.95	no-noise
EM	$T_{max} = 1.5\text{K}$	8	8	9	10	8
	$T_{max} = 2.0\text{K}$	6	7	7	8	6
FM	$T_{max} = 1.5\text{K}$	7	9	8	9	8
	$T_{max} = 2.0\text{K}$	6	7	7	7	7
MM	$T_{max} = 1.5\text{K}$	7	8	(4)	—	8
	$T_{max} = 2.0\text{K}$	6	7	7	8	7

Table 7. Difference of PNR between strong and no negative emissions. Values in parentheses if no PNR exists without negative emissions, PNR is then assumed to have been 2015.



Appendix: SCB and PNR Parameter Sensitivity

SCB and PNR sensitivities were determined by varying each parameter by $\pm 10\%$ and running the calculation to see how the obtained value changes. Sensitivities were determined for all discussed 465 values of T_{max} , β , and the EM, FM and MM scenarios in case of PNR. We show (Table 8) sample values for a small ($T_{max} = 1.5\text{K}$, $\beta = 0.95$), intermediate ($T_{max} = 1.5\text{K}$, $\beta = 0.5$), and large ($T_{max} = 2.0\text{K}$, $\beta = 0.5$) SCB, corresponding to a close, intermediate and far PNR.

The biggest effects on the SCB are found for the initial condition of the large carbon reservoirs and the radiative forcing parameters A , α and C_0 that are essentially fixed constants. The parameters 470 of the carbon model (a_i, τ_i) do not have big impacts on the found SCB, on the order of 0 – 17 GtC, with the larger numbers found for larger absolute values of SCB. Varying the temperature-model parameters can have quite noticeable effects, up to 10% for large and up to 50% for small values of SCB. The model is particularly sensitive to changes in the intermediate timescale (b_2, τ_{b2}). Likely, possible variations in the (model) parameters are not independent, potentially canceling each other. 475 The sensitivity of SCB and PNR to the noise amplitudes is small, with largest values found for the multiplicative noise amplitude that is responsible for much of the spread of the temperature distribution (so increasing σ_{T2} decreases the SCB).

The PNR sensitivities are generally small and in no way change our message qualitatively. The effect of initial conditions and carbon model parameters is small, often even unnoticeable (with the 480 exception of the permanent carbon reservoir, due to its large size). We find the most relevant, yet small, sensitivities in the temperature model parameters. For example, a 10% error in τ_{b2} can move the PNR by 2-3 years. An interesting effect is the case of r_γ , the energy-saving progress (reduction in energy-intensity of a unit of economic output and in effect equivalent to a decrease in the emission growth rate) which is taken zero by default. Increasing it to 1% or 2% has little effect on *close* PNR 485 (e.g. 2020) but is capable of delaying *late* PNR by up to 15 years, and the effect is more substantial for the less ambitious scenarios. This is an interesting finding, showing that in the long run increasing energy efficiency can play a role in avoiding the PNR.



	SCB			PNR		
T_{max}, β	1.5K, 0.95	1.5K, 0.5	2.0K, 0.5	1.5K, 0.95	1.5K, 0.5	2.0K, 0.5
undisturbed	68.63	247.02	492.09	2022	2036	2050
C_1	15.06, -15.01	14.75, -14.48	14.65, -13.41	2, -1	1, -1	1, 0
C_2	1.59, -2.07	1.96, -2.0	1.47, -1.88	0, 0	0, 0	0, 0
ΔT_1	-0.12, -0.05	0.09, -0.0	0.52, 0.04	0, 0	0, 0	0, 0
ΔT_2	-0.04, -0.03	0.05, 0.1	-0.04, -0.49	1, 0	0, 0	0, 0
a_1	2.81, -2.82	10.24, -9.41	19.52, -17.2	0, 0	0, -1	1, -1
a_2	0.68, -0.79	3.27, -2.91	7.76, -6.49	1, 1	0, -1	1, 0
τ_1	3.64, -3.02	4.73, -3.75	5.92, -4.43	0, 0	0, 0	1, 0
τ_2	4.58, -4.48	7.6, -7.1	12.44, -11.08	1, 0	0, -1	1, 0
A	55.59, -44.99	80.98, -64.43	118.57, -93.23	5, -4	5, -5	6, -5
α	55.76, -44.97	80.91, -64.52	118.18, -92.85	5, -4	5, -5	6, -5
C_0	-, 169.67	-188.37, 182.48	-205.7, 199.12	-, 13	-15, 11	-12, 10
b_1	12.17, -11.57	22.74, -21.04	32.55, -31.19	1, -1	2, -2	2, -1
b_2	32.08, -28.29	38.94, -34.41	57.89, -50.29	4, -2	2, -3	3, -2
τ_{b1}	12.31, -11.83	23.02, -21.17	34.51, -30.64	1, -1	1, -2	2, -1
τ_{b2}	37.84, -33.21	38.13, -33.51	56.77, -49.36	4, -3	2, -3	3, -2
γ_0	~, ~	~, ~	~, ~	1, -1	2, -2	3, -2
r_γ	~, ~	~, ~	~, ~	1, 1	2, 5	6, 15
σ_{T2}	10.04, -10.16	-3.0, 3.55	-4.68, 5.15	1, -1	0, 0	0, 0

Table 8. Sensitivity of Safe Carbon Budget and Point of No Return to parameter variations. Values as difference in GtC (SCB) and number of years (PNR) from the undisturbed value (first row). The PNR values all refer to the EM scenario. First and second numbers give 10% parameter decrease and increase, respectively. Exception is r_γ (in orange) which is zero by default and where first and second numbers give $r_\gamma = 0.01$ and $r_\gamma = 0.02$, respectively. No sensitivities are calculated for the SCB for the economic parameters γ_0 and r_γ and replaced by (~), whereas (–) implies no positive SCB/PNR could be calculated. The fields corresponding to the radiative forcing parameters A, α, C_0 are colored in cyan, while the most sensitive climate model parameters b_2, τ_{b2} are given in orange.